Inorg. Chem. **2007**, *46*, 4256–4266

Two-Dimensional Heisenberg Antiferromagnets: Syntheses, X-ray Structures, and Magnetic Behavior of $[Cu(pz)_2](ClO_4)_2$, $[Cu(pz)_2](BF_4)_2$, and $[Cu(pz)_2(NO_3)](PF_6)$

F. Matthew Woodward,[†] Pamela J. Gibson,[‡] Geoffrey B. Jameson,[§] Christopher P. Landee,[†] Mark M. Turnbull,*[,‡] and Roger D. Willett[||]

Department of Physics and Carlson School of Chemistry and Biochemistry, Clark University, 950 Main Street, Worcester, Massachusetts 01610, Department of Chemistry, Institute of Fundamental Sciences, Massey University, Palmerston North, New Zealand, and Department of Chemistry, Washington State University, Pullman, Washington 99164

Received November 10, 2006

We report on the syntheses, crystal structures, and magnetic susceptibilities of a family of copper pyrazine (pz)-based antiferromagnets with moderate in-plane magnetic exchange. These materials fall into two classes: monoclinic complexes $[Cu(pz)_2]A_2$ for $A = ClO_4$ (**1**) or BF_4 (**2**) and the tetragonal complex $[Cu(pz)_2(NO_3)]PF_6$ (**3**). Compound **1** and its deuterated version $[Cu(pz\text{-}d_4)_2](ClO_4)_2$ (**1a**) crystallize in the space group *C*2/*m* at room temperature with disordered perchlorate anions. For both **1** and **2**, the *C* centering of the Cu(II), $S = {}^1/_2$, site yields four equivalent nearest neighbors, producing layers of Cu(II) ions bridged by the pz molecules, which map onto a square magnetic lattice. The layers are offset such that Cu(II) ions lie above and below the holes of adjacent layers. Compound **3** crystallizes in the space group *I*4/*mcm* with a layer structure similar to those of **1** and **2** but with Cu(II) ions of adjacent layers stacked above each other and bridged by semicoordinate NO_3^- ions. The variable-temperature susceptibilities in these compounds approximate a two-dimensional Heisenberg antiferromagnet with *J* values within the layers of 17.5(3) K (**1**), 15.3(3) K (**2**), and 10.8(3) K (**3**). Ordering transitions are observed in the magnetic data at 4.2(3) and 4.3(5) K for **1** and **2**, respectively.

Introduction

Copper coordination compounds have been an important component in the development of molecular-based chemistry over the past quarter century.[1] The d^9 configuration of the Cu(II) ion has one unpaired electron, rendering Cu(II) an $S = {}^1/_2$ ion. The nearly complete quenching of the orbital angular momentum provides an average *g* factor close to 2, indicating the absence of any large internal magnetic fields. This combination of features makes Cu(II) compounds excellent examples of Heisenberg ions (in which moments are free to follow an external field) in the small spin number (or quantum spin) limit. For similar reasons, the Mn(II) ion can be described as a Heisenberg ion in the large spin number (or classical spin) limit.

The discovery[2] of high-temperature superconductors 2 decades ago in the two-dimensional (2D) copper oxide compounds gave rise to a strong interest in the properties of 2D $S = {}^1/_2$ Heisenberg antiferromagnets (2D QHAF), particularly after a leading theory[3] explained the high superconducting critical temperature as arising from the strong ($J/k \approx 1500$ K) exchange interactions present in the copper oxides. The copper oxides have been extensively studied,[4] both as the insulating, undoped materials such as La_2CuO_4 and as the superconducting, doped compounds such as $La_{2-x}Sr_xCuO_4$. All of the studies of the copper oxides have

* To whom correspondence should be addressed. E-mail: mturnbull@clarku.edu (M.M.T.), clandee@clarku.edu (C.P.L.).
[†] Department of Physics, Clark University.
[‡] Carlson School of Chemistry, Clark University.
[§] Massey University.
[||] Washington State University.

(1) (a) Hendrickson, D. N. In *Magneto−Structural Correlations in Exchange Coupled Systems*; Willett, R. D., Gatteschi, D., Kahn, O., Eds.; Reidel Publishers: Dordrecht, The Netherlands, 1985; pp 555−602. (b) The papers in *Polyhedron* **2005**, *24* and the previous proceedings of the International Conferences on Molecule-Based Magnets.

(2) For a review, see: Kastner, M. A.; Birgeneau, R. J.; Shirane, G.; Endoh, Y. *Rev. Mod. Phys.* **1998**, *70*, 897.

(3) (a) Anderson, P. W. *Science* **1987**, *253*, 1196. (b) Manousakis, E. *Rev. Mod. Phys.* **1991**, *63*, 1. (c) Coleman, P. *J. Magn. Magn. Mater.* **1989**, *82*, 159.

10.1021/ic0621392 CCC: $37.00
Published on Web 04/14/2007

been done in the limit of small applied magnetic fields ($g\mu_B SH \ll JS^2$) because an exchange strength of $J/k \approx 1500$ K corresponds to an applied field of over 4000 T. An increasing number of theoretical studies of the 2D QHAF in applied fields have indicated that dramatic changes appear in the energy spectrum for these magnets as applied fields approach the saturation fields,[5] but confirmation of these predictions will not be possible in the copper oxides. (In this report, we discuss all interaction strengths in terms of the positive single J Hamiltonian, $H = J\sum_{nn} S_i \cdot S_{i+1}$, where the sum of the interactions is to the four nearest neighbors. Note that for this choice of Hamiltonian a positive exchange strength corresponds to antiferromagnetic interactions.)

We have turned to copper coordination complexes to create new compounds that are good representations of 2D QHAF with exchange strengths small enough to be overcome with accessible fields. These compounds must contain Cu(II) ions with four equivalent antiferromagnetic interactions to neighboring metal sites within the layers and minimal interactions between layers. The intralayer requirements can be satisfied by locating the Cu(II) ions on sites of 4-fold symmetry or by having adjacent Cu(II) ions related by *C* centering. The latter possibility was found in the three tetrabromocuprate compounds A_2CuBr_4, where A is a five-substituted 2-aminopyridinium molecule such as 5-methyl-2-aminopyridinium.[6] In these compounds, the relatively weak interlayer interactions arose through bromide−bromide contacts[7] ($J/k = 8.5$ K (5-chloro), 6.5 K (5-methyl), 6.9 K (5-bromo)), permitting the low-temperature magnetizations of these compounds to be driven to saturation by external fields of 24, 19, and 20 T, respectively.[6] There are also bromide−bromide contacts between the layers that lead to relatively high three-dimensional (3D) ordering temperatures of 5.1, 3.8, and 4.0 K, respectively.[6] To fully understand the behavior of 2D QHAF without the complications of significant interlayer interactions J', it is necessary to find materials with lower J'/J ratios. The current study describes the properties of a family of 2D QHAF based upon the general formula $Cu(pz)_2A_2$ (where A represents a noncoordinating or poorly coordinating anion and pz is pyrazine, $C_4H_4N_2$).

Copper pyrazine compounds provide an excellent starting point for this process as they are known throughout the literature to form linear chains[8] and layered structures,[9] with the pz molecule linking Cu atoms in large coordination polymers. The parent compound for this work, $[Cu(pz)_2](ClO_4)_2$,[10] consists of *C*-centered Cu layers with each Cu connected to its nearest neighbors by four equivalent pz molecules. Initial powder magnetic susceptibility data showed the compound to possess moderate antiferromagnet interactions ($J \sim 15$ K). The structure and reported magnetic behavior of $[Cu(pz)_2](ClO_4)_2$ led us to explore the preparation of similar compounds based on the chemical formula $[Cu(pz)_2]A_2$ so as to produce a family of 2D Heisenberg antiferromagnets that would allow study of the structure/magnetic superexchange relationships. The long semicoordinate bond between the ClO_4^- ion and the Cu ion provides good spatial isolation between the Cu−pz layers, suggesting that similar poorly coordinating anions might provide similar structures. To this end, we have prepared two analogues, the tetrafluoroborate salt and the mixed-anion complex $[Cu(pz)_2(NO_3)]PF_6$, and report here their syntheses, structures, and magnetic properties.

Experimental Section

Acids, pyrazine, and pyrazine-d_4 were purchased from Aldrich Chemical and used as received. Metal salts were purchased from Alfa-Aesar and dried under vacuum prior to use. IR spectra were taken on a Perkin-Elmer Paragon 500 spectrophotometer.

Synthesis. $[Cu(pz)_2](ClO_4)_2$ (1). $Cu(ClO_4)_2 \cdot 6H_2O$ (1.85 g, 5 mmol) and pz (0.80 g, 10 mmol) were dissolved in 20 mL of H_2O, and a drop of dilute $HClO_4$(aq) was added to prevent precipitation of $Cu(OH)_2$ or $CuCO_3$. The solution was then partially covered and left to evaporate. Crystals of **1** grew over a period of several weeks. The mixture was filtered, and the recovered crystals were washed with a small amount of cold H_2O and left to air-dry to give 1.02 g (24%). No attempt was made to maximize the yield. IR (KCl): ν 3120w, 1420s, 1150s, 1105vs, 1086vs, 802 m, 622s, 489m cm^{-1}.

The compounds $[Cu(pz\text{-}d_4)_2](ClO_4)_2$ (**1a**) and $[Cu(pz)_2](BF_4)_2$ (**2**) were made in a similar fashion on the same or slightly larger scales. Yield for **1a**: 2.0 g (50%). IR (KCl): ν 2315w, 2290w, 1285s, 1146vs, 1113vs, 1084vs, 870m, 626s, 456m cm^{-1}. Yield for **2**: 1.27 g (64%). IR (KCl): ν 3140w, 1420s, 1114vs, 1066vs, 1032vs, 802s, 491m cm^{-1}.

$[Cu(pz)_2(NO_3)]PF_6$ (3). $Cu(NO_3)_2 \cdot 3H_2O$ (0.725 g, 3.0 mmol) and pz (0.48 g, 6.0 mmol) were dissolved in 15 mL of H_2O. KPF_6 (1.66 g, 9.0 mmol) was dissolved in 5 mL of H_2O and added with stirring. A blue precipitate (ppt) formed rapidly and was removed by filtration. The ppt was rinsed with cold H_2O and allowed to air-dry. Yield: 1.00 g (62%). IR (KCl): ν 3150w, 3061w, 1437m, 1328m, 840vs, 560s, 490m cm^{-1}. Crystals suitable for X-ray diffraction were grown by slow evaporation of the filtrate. Powder X-ray diffraction data verified that the initial precipitate was the same material as that used for the single-crystal studies.

(4) (a) Hayden, S. M.; Aeppli, G.; Osborn, R.; Taylor, A. D.; Perring, T. G.; Cheong, S. W.; Fisk, Z. *Phys. Rev. Lett.* **1991**, *67*, 3622. (b) Greven, M.; Birgeneau, R. J.; Endoh, Y.; Kastner, M. A.; Keimer, B.; Matsuda, M. Shirane, G.; Thurston, T. R. *Phys. Rev. Lett.* **1994**, *72*, 1096.

(5) (a) Zhitomirsky, M. E.; Chernyshev, A. L. *Phys. Rev. Lett.* **1999**, *82*, 4536. (b) Syljuåsen, O. F.; Lee, P. A. *Phys. Rev. Lett.* **2002**, *88*, 207207.

(6) (a) Woodward, F. M.; Albrecht, A. S.; Wynn, C. M.; Landee, C. P.; Turnbull, M. M. *Phys. Rev. B: Condens. Matter Mater. Phys.* **2002**, *65*, 14412: 1−13. (b) Matsumoto, T.; Miyazaki, Y.; Albrecht, A. S.; Landee, C. P.; Turnbull, M. M.; Sorai, M. *J. Phys. Chem. B* **2000**, *104*, 9993. (c) Woodward, F. M.; Landee, C. P.; Giantsidis, J.; Turnbull, M. M.; Richardson, C. *Inorg. Chim. Acta* **2001**, *324*, 324.

(7) Turnbull, M. M.; Landee, C. P.; Wells, B. M. *Coord. Chem. Rev.* **2005**, *249*, 2567.

(8) (a) Santoro, A.; Mighell, A. D.; Reimann, C. W. *Acta Crystallogr.* **1970**, *B26*, 979. (b) Richardson, H. W.; Hatfield, W. *J. Am. Chem. Soc.* **1976**, *98*, 835. (c) Amaral, S.; Jensen, W. E.; Landee, C. P.; Turnbull, M. M.; Woodward, F. M. *Polyhedron* **2001**, *20*, 1317. (d) Otieno, T.; Gipson, A. M.; Parkin, S. *J. Chem. Crystallogr.* **2002**, *32*, 81.

(9) (a) Lumme, P.; Lindroos, S.; Lindell, E. *Acta Crystallogr., Sect. C* **1987**, *43*, 2053. (b) Kitagawa, S.; Munakata, M.; Tanimura, T. *Inorg. Chem.* **1992**, *31*, 1714. (c) Otieno, T.; Rettig, S. J.; Thompson, R. C.; Trotter, J. *Inorg. Chem.* **1993**, *32*, 1607 and 4384. (d) Turnbull, M. M.; Pon, G.; Willett, R. D. *Polyhedron* **1991**, *15*, 1835.

(10) Darriet, J.; Haddad, M. S.; Duesler, E. N.; Hendrickson, D. N. *Inorg. Chem.* **1979**, *18*, 2679.

Table 1. Crystallographic Data and Structure Refinement Details for **1**−**3**

	1 (293 K; 163 K)	**1a**	**2**	**3**
formula	$C_8H_8N_4O_8Cl_2Cu$	$C_8D_8N_4O_8Cl_2Cu$	$C_8H_8B_2N_4F_8Cu$	$C_8H_8N_5O_3F_6OCu$
fw	422.62	430.67	397.34	430.70
cryst size, mm^3	0.08 × 0.08 × 0.08; 0.13 × 0.44 × 0.76	0.30 × 0.41 × 0.44	0.15 × 0.20 × 0.50	0.18 × 0.35 × 0.60
cryst syst	monoclinic	monoclinic	monoclinic	tetragonal
space group	*C*2/*m*; *C*2/*c*	*C*2/*c*	*C*2/*m*	*I*4/*mcm*
a, Å	9.734(2); 14.072(5)	14.045(5)	9.692(2)	9.7093(11)
b, Å	9.729(2); 9.786(3)	9.759(3)	9.736(2)	9.7093(11)
c, Å	8.1320(17); 9.781(3)	9.800(3)	7.916(2)	14.0055(19)
β, deg	120.855(4); 96.458(4)	96.491(4)	120.920(10)	90.00
V, $Å^3$	661.1(2); 1338.3(7)	1334.6(8)	640.8(2)	1320.3(3)
Z	2; 4	4	2	4
T, K	293(2); 163(2)	163(2)	160(2)	163(2)
ρ_{calc}, Mg/m^3	2.123; 2.098	2.143	2.059	2.167
μ(Mo Kα), mm^{-1}	2.109; 2.084	2.089	1.804	1.876
max/min trans	0.8494; 1.000−0.412	1.000−0.726	0.567−0.531	0.412−0.303
reflns collected	2985; 7980	8026	544	623
unique reflns	991; 1417	1379	534	340
data/restraints/params	991/0/77; 1417/0/117	1379/0/117	534/9/66	340/62/80
GOF	1.056; 1.107	1.208	1.117	1.175
R1, wR2 [$I > 2\sigma(I)$]	0.0311, 0.0791; 0.0600, 0.1543	0.0338, 0.0952	0.0372, 0.1021	0.0360, 0.0896
R1,[a] wR2[b] (all data)	0.0331, 0.0801; 0.0614, 0.1556	0.0341, 0.0954	0.399, 0.1041	0.0451, 0.0935
max/min peaks, $e/Å^3$	0.483/−0.231; 2.508/−1.312	0.901/−0.842	0.682/−0.598	0.350/−0.450

[a] $R1 = \sum|F_o - F_c|/\sum|F_o|$. [b] $wR2 = \sum(F_o^2 - F_c^2)^2/\sum w(F_o^2)^{1/2}$.

X-ray Structures. X-ray data were collected for both **1** and **1a** by mounting single crystals on a thin glass fiber and placing them on a Bruker CCD diffractometer with monochromatic Mo Kα radiation. Cell parameters were retrieved using SMART[11] software and refined using SAINTPlus[12] on all observed reflections. Data reduction and correction for Lorentz polarization and decay were performed using the SAINTPlus software. Absorption corrections were applied using SADABS.[13] The structures were solved by direct methods and refined by the least-squares method on F^2 using the SHELXTL program package.[14] Data for **2** and **3** were collected on a Siemens P4 diffractometer also employing Mo Kα radiation and a graphite monochromator. Data reductions, structure solutions, and refinements were carried out using SHELXTL software.[15] Structures were solved using SHELXS93[16] and refined via SHELXL93.[17] Data collection and refinement details are given in Table 1. Selected bond lengths and angles are given in Table 2.

Additional Details for 3. The PF_6 ion was badly disordered, with the central P atom occupying two distinct sites and the peripheral F atoms at one of the PF_6 sites additionally disordered. Although one site is located at a special position, the entire PF_6 group was entered as a rigid group. Bond length and bond angle restraints were imposed by means of a free variable. EADP constraints were used to enforce identity on crystallographically independent F sites in close proximity (closer than 1 Å) and on those related by crystallographic symmetry. SUMP restraints were used to ensure that the total occupancy over the two sites was one PF_6. Isotropic displacement parameters were used for all F atoms. The absence of significant residual electron density in the vicinity of the PF_6 moiety indicates that this model has accounted for the electron density at the site in a chemically sensible manner. The NO_3 moiety is also (crystallographically) disordered. There are apparently unnaturally close contacts between the NO_3 and PF_6

Table 2. Selected Bond Lengths (Å) and Angles (deg) for **1**−**3**[c]

	1 (293 K)	**1** (163 K)	**1a**	**2**	**3**
		Lengths			
Cu−N1	2.0514(14)	2.071(3)	2.064(2)	2.042(3)	2.042(4)
Cu−N2		2.074(3)	2.064(2)		
Cu−X	2.361(2)	2.374(3)	2.369(2)	2.338(3)	2.413(5)
N1−C1	1.332(2)	1.340(5)	1.345(4)	1.337(5)	1.329(4)
N1−C2				1.342(5)	
N1−C3		1.344(4)	1.344(4)		
N2−C2		1.343(5)	1.344(4)		
N2−C4		1.345(4)	1.347(4)		
C1−C2	1.378(2)			1.375(6)	1.380(7)
C1−C3		1.386(5)	1.388(4)		
C2−C4		1.386(5)	1.381(4)		
		Angles			
N1−Cu−N1[a]	89.06(8)	89.27(16)	88.78(13)	89.08(16)	90.0
N1−Cu−N2			91.10(13)	90.89(10)	
N1−Cu−N2[b]		179.42(9)	179.46(8)		
N2−Cu−N2[a]		88.54(16)	89.45(13)		
N1−Cu−X	89.22(6)	87.53(10)	87.80(8)	90.23(10)	90.0
N2−Cu−X			90.97(10)	91.78(8)	
Cu−X−Y	167.54(13)	159.90(18)	160.07(14)	161.9(5) 166.6(6)	159.6(6)

[a] Symmetry transformations. **1** (293 K): $-x + 1, y, -z + 1$. **1** (163 K): $-x, y, -z + 1/2$. [b] Symmetry transformations. **2**: $-x, -y + 2, -z$. [c] X = O or F, Y = Cl or B.

(11) SMART, version 5.626, Bruker Molecular Analysis Research Tool; Bruker AXS, Inc.: Madison, WI, 2002.
(12) SAINTPlus, version 6.36a, Data Reduction and Correction Program; Bruker AXS, Inc.: Madison, WI, 2001.
(13) Sheldrick, G. M. SADABS, version 1.02, An Empirical Absorption Correction Program; Bruker AXS, Inc.: Madison, WI, 2002.
(14) Sheldrick, G. M. SHELXTL, version 6.10, Structure Determination Software Suite; Bruker AXS, Inc.: Madison, WI, 2001.
(15) Sheldrick, G. SHELXTL/PC; Siemens Analytical X-ray Instruments, Inc.: Madison, WI, 1990.
(16) Sheldrick, G. M. *Acta Crystallogr., Sect. A* **1990**, *46*, 467.
(17) Sheldrick, G. M. SHELXL93, Program for the Refinement of Crystal Structures; University of Göttingen: Göttingen, Germany, 1993.

moieties. However, these contacts are an artifact of the assumption that disorder of the NO_3 moiety is uncorrelated with disorder of the PF_6 moiety.

Crystallographic data for the structures have been deposited with the Cambridge Crystallographic Data Centre as supplementary publications no. CCDC-203408 (**1**, 293 K), CCDC-203407 (**1**, 163 K), CCDC-203406 (**1a**), CCDC-240379 (**2**), and CCDC-240378 (**3**). Copies of the data can be obtained from the CCDC, 12 Union Road, Cambridge CB2 1EZ, U.K. (fax, int. code + 44(1223)336-033; e-mail, deposit@ccdc.cam.ac.uk).

Magnetic Measurements. Magnetic susceptibility data were collected using Quantum Design MPMSR2 and MPMS-XL SQUID magnetometers. For all compounds, the first study was an isothermal magnetization at 1.8 K in fields of up to 5 T. Evidence of weak upward curvature in the data sets was found for all compounds. Temperature-dependent magnetization was collected for all compounds in a field of 0.1 T from 1.8 to 325 K. The correction used for the temperature-independent paramagnetic response of Cu was 60×10^{-6} cm^3/mol. Corrections for the temperature-independent diamagnetic response of the samples are -179×10^{-6}, -184.2×10^{-6}, and -185.5×10^{-6} cm^3/mol for **1**, **2**, and **3**, respectively.[18] The diamagnetic contribution of the sample holder was subtracted separately.

Results

Synthesis. Compounds **1** and **2** were prepared by the reaction of the corresponding copper salt $Cu(ClO_4)_2 \cdot 6H_2O$, $Cu(BF_4)_2 \cdot 6H_2O$ with 2 equiv of pz or pz-d_4 in aqueous solution. Crystals of the complexes $Cu(pz)_2A_2$ (A = ClO_4 or BF_4) grew over the course of several weeks. Compound **3** was prepared by the reaction of $Cu(NO_3)_2 \cdot 3H_2O$ with 2 equiv of pz in the presence of an excess of KPF_6 in aqueous solution. Again, crystals grew over a period of several weeks. All compounds produced crystals suitable for single-crystal X-ray analysis.

Structure. $[Cu(pz)_2](ClO_4)_2$ crystallizes in the space group *C*2/*m* at room temperature and in the space group *C*2/*c* at 163 K. The phase change appears to be completely reversible and is believed to occur near 180 K as determined by infrared spectroscopy.[19] The local coordination geometry of **1** for both phases is shown in Figure 1. Each Cu(II) ion is coordinated to four pz molecules, each of which bridges to another Cu(II) ion. The differences between the two *C*-centered structures lie in the details of the crystallographic packing and the formation of the $Cu(pz)_2$ layers.

In the *C*2/*m* structure, the copper ion is located at the cell origin, both a crystallographic mirror and a 2-fold axis. The four pyrazine molecules are divided into two identical pairs related via the 2-fold axis and mirror plane. One pair of *cis*-pyrazine molecules is canted in a positive fashion, 65.8°, and the other pair is canted in the opposite fashion at an angle of −65.8° (Table 3), with respect to the Cu−N plane (see Figure 1). This Cu−pz configuration is then repeated via the *C* centering to generate the Cu−pz layer (Figure 2a). The Cu−pz−Cu linkages lie along the diagonals of the *ab* faces. In this way, every copper site is connected to each

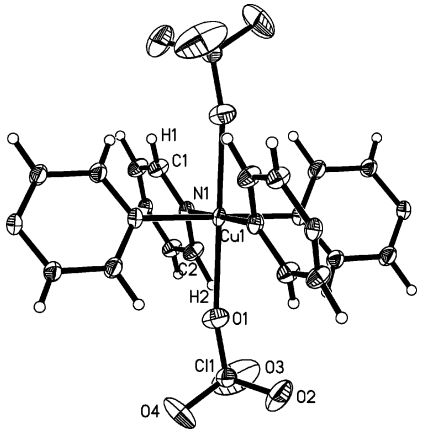

Figure 1. Thermal ellipsoid plot (50%) of $[Cu(pz)_2](ClO_4)_2$ at room temperature showing the four coordinated pz molecules. H atoms are shown as arbitrary spheres. Only the asymmetric unit has been labeled, and only one position of the disordered ClO_4 ions is shown for clarity.

Table 3. Canting Angles (deg) in **1**−**3**

compound	canting angle	compound	canting angle
1 (rt)	65.8	**2** (160 K)	67.4
1 (160 K)	69.1, 62.8	**3** (160 K)	61.4
1a (160 K)	69.0, 62.6		

adjacent copper site by an identical pyrazine molecule 2.781 Å long (measured from nitrogen to nitrogen). The Cu to pz−N bond is 2.051 Å, giving a total distance of 6.881 Å between Cu ions within a given layer.

The ClO_4 ions at room temperature are semicoordinate ($d_{Cu-O} = 2.361(2)$ Å) and show two-site disorder with respect to the crystallographic mirror. Within the ClO_4 tetrahedra, the oxygen atom that is coordinated to the copper atom (O1) and a second oxygen atom (O2) sit on the [010] mirror and are shared by the two disordered positions. The two remaining O atoms and the Cl atom in the ClO_4 tetrahedra are shifted off the mirror plane, resulting in the observed two-site disorder. This treatment of the disorder is different from that of Darriet et al.[10] but results in a better refinement and more reasonable bond angles about the chlorine atom.

The ClO_4 ions lie between the planes in the space framed by four pz molecules of the adjacent layer. This ball (ClO_4 ion)-and-cup (made of tilted pz molecules) arrangement is seen in Figure 3 where the ClO_4 ion coordinated to the adjacent layer is shown surrounded by pz molecules. Also implicit in Figure 3 is the offset of Cu atoms between the Cu−pz layers. This structural arrangement yields a packing with a large distance between layers (6.98 Å as measured from the Cu−pz plane to the Cu−pz plane) and an even greater distance between individual Cu sites (the closest interplane Cu−Cu distance is 8.54 Å).

The differences in the coordination sphere about the Cu ions between the *C*2/*m* (high temperature) and *C*2/*c* (low temperature) structures are minor and mostly related to the ordering of the ClO_4 units and the canting of the pz rings. The *C*2/*c* structure has no mirror plane passing through the Cu as in the *C*2/*m* structure. This is the result of a change in the tilt angle of the pz molecules relative to the Cu−pz plane. In this case, rather than two pairs of identical *cis*-pz molecules having a tilt of ±65.8°, one pair has a tilt angle

(18) Carlin, R. L. *Magnetochemistry*; Springer-Verlag: Berlin, 1986.
(19) Choi, J.; Woodward, J. D.; Musfeldt, J. L.; Landee, C. P.; Turnbull, M. M. *Chem. Mater.* **2003**, *15*, 2797.

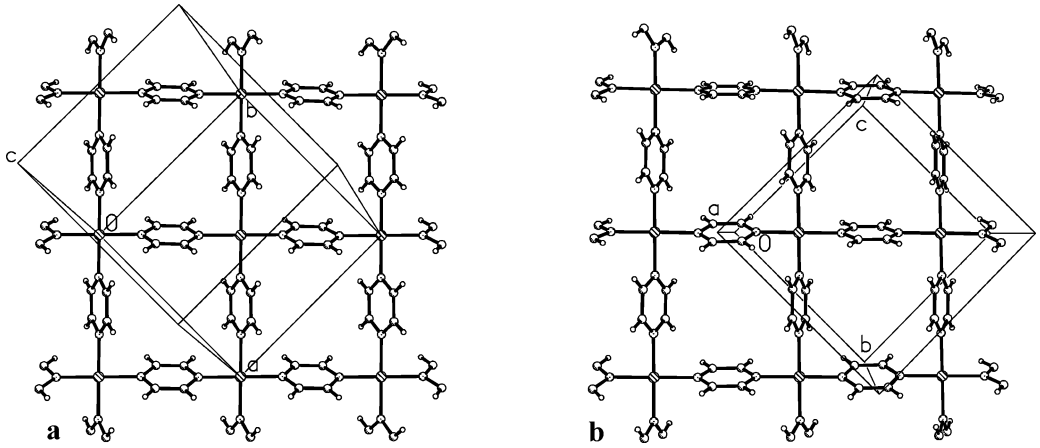

Figure 2. Layer structure of $[Cu(pz)_2](ClO_4)_2$ at (a) 293 K and (b) 163 K. Part a is shown perpendicular to the *ab* plane whereas part b is shown perpendicular to the *bc* plane. The ClO_4 ions have been removed for clarity.

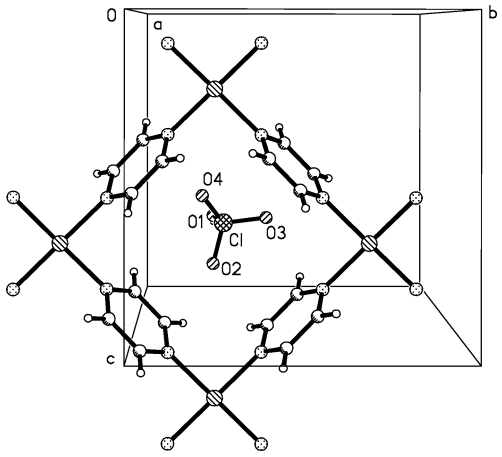

Figure 3. Ball-and-cup relationship of the ClO_4 ions of one layer to the cavity formed by the pz molecules of the next layer.

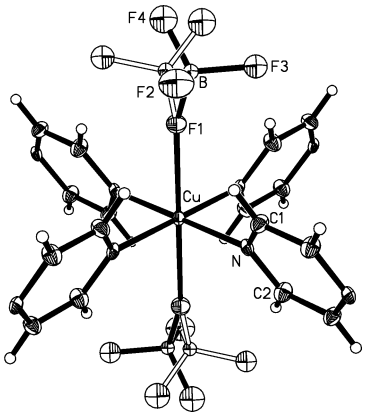

Figure 4. Thermal ellipsoid plot of **2** showing the disorder of the BF_4 anions. Only the asymmetric unit is labeled. H atoms are shown as spheres of arbitrary size.

of +62.8° and a Cu−N1 distance of 2.071 Å whereas the other pair has a tilt of −69.1° and a slightly longer Cu−N2 distance of 2.074 Å. This change in the pz tilt angle has little effect on the nearest-neighbor Cu distances within the plane. The pz molecule tilted by 62.8° has a length of 2.77 Å with a Cu−N bond of 2.07 Å for an overall nearest-neighbor Cu distance of 6.92 Å, showing very little difference from the second pz molecule tilted by 69.1°, which has a length of 2.78 Å with a Cu−N bond length of 2.07 Å for a total Cu−Cu distance also of 6.92 Å. The other change in local structure upon going from *C*2/*m* to *C*2/*c* is observed in the ClO_4 ions. The ClO_4 ions are no longer disordered and are now related to one another by the *c*-glide operation. The same ball-and-cup relationship occurs between planes.

The major change in the structure at lower temperatures is found in the formation of the Cu−pz layers and their relationship to the unit cell. Figure 2b shows one Cu−pz layer viewed perpendicular to the *bc* plane. The copper is located in the unit cell at (0, 0.7499(1), 0.25), rendering *y* and −*y* nearly identical positions. Here, the copper ions are related by the *c*-glide operation rather than by the *C* centering. The *C*-centering operation in this structure results in the formation of adjacent Cu−pz layers. Thus, at room temperature, the Cu−pz planes are formed via the *C* centering and lie parallel to the *ab* face, whereas at low temperature, the layers are formed via the *c*-glide plane and lie parallel to the *bc* plane.

The structure of the deuterated analogue, **1a**, was also determined at 163 K. The two compounds are isomorphous at that temperature and show negligible differences in their cell constants. Bond lengths and angles are nearly identical between the two compounds, within experimental error, with the exception of the N1−Cu−N1A bond angle, which has decreased slightly. The N···N distances within the pz rings are both 2.79 Å, comparable to those of **1**, and the ring canting angles (62.6° for the N1 ring, −69.0° for the N2 ring) are also comparable to those of **1**.

Compound **2**, the tetrafluoroborate analogue, crystallizes in the space group *C*2/*m* at 163 K and is shown in Figure 4. It is isomorphous with the room-temperature structure of **1**. The same type of disorder for the BF_4 anions is seen in the structure of **2** as was observed for the ClO_4 ions in the room-temperature structure of **1**. The N···N separation within a pz ring is 2.78 Å which, coupled with the slightly shortened Cu−N bond length of 2.04 Å, leads to Cu···Cu separations within a layer of 6.87 Å. The distance between a Cu atom and the mean plane of the adjacent layer is 6.79 Å, and the closest Cu···Cu distance between planes is 7.92 Å. The ring canting angles are 67.4°.

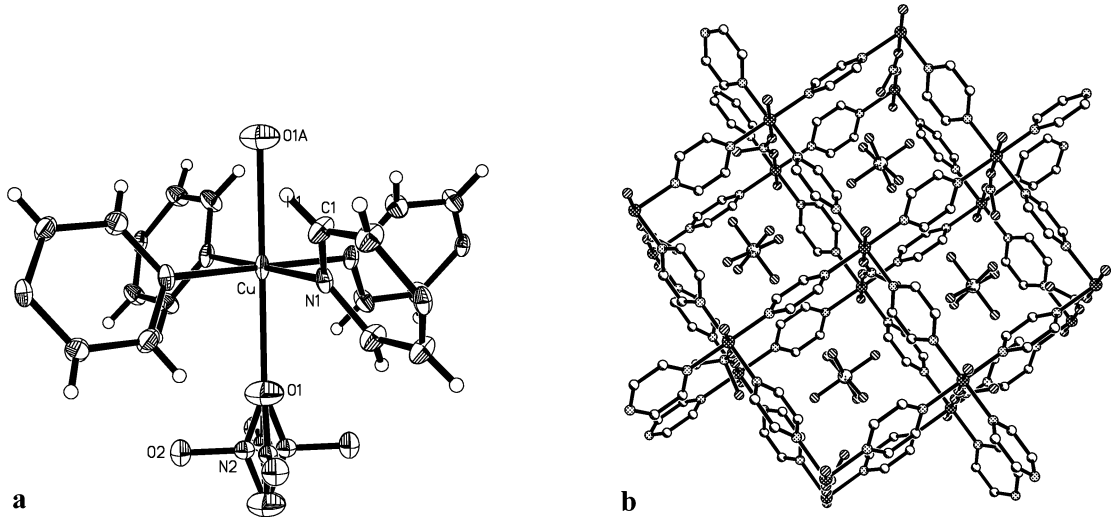

Figure 5. (a) Thermal ellipsoid plot of the coordination sphere of **3**. The asymmetric unit and the additional coordinated nitrate O atom are labeled. The 4-fold disorder of the NO_3^- ions is shown. H atoms are shown as spheres of arbitrary size. (b) Packing diagram of **3** showing the 3D structure. Only one position for each disordered PF_6 and NO_3 ion is shown. H atoms have been removed for clarity.

Compound **3** is distinct from the ClO_4 and BF_4 analogues. It crystallizes in the tetragonal space group *I*4/*mcm* and has mixed anions, one NO_3^- and one PF_6^- per Cu(II). The structure is shown in Figure 5a, and the packing is shown in Figure 5b.

Compound **3** also forms as 2D layers of Cu ions bridged by pz molecules, but unlike **1** and **2** where adjacent Cu−pz layers were offset, here they lie directly above one another and are linked by bridging semicoordinate NO_3^- ions, creating boxes. The PF_6 ions lie in the boxes so formed and are highly disordered (see the Experimental Section for treatment of the disorder). The NO_3^- ions show 4-fold disorder due to the tetragonal structure. The N···N separation within a pz ring (2.78 Å) and the Cu−N bond length (2.04 Å) are the same as those seen in **2**, as is the Cu···Cu separation within a layer (6.87 Å). The distance between Cu atoms, and hence the closest interplane Cu···Cu distance, is 7.00 Å, significantly shorter than that seen in either **1** or **2**. The canting angle for the pz rings (61.4°) is the smallest seen in any of the compounds studied.

Magnetism. The susceptibilities of all three compounds (Figure 6a) show rounded maxima below 20 K, characteristic of low-dimensional antiferrromagnetic behavior.[20] The antiferromagnetic nature of the dominant interactions is confirmed by comparing the data sets above 40 K to the Curie−Weiss expression. The Curie−Weiss temperatures (θ_{CW}) were found to be −23.8(3), −22.3(3), and −14.0(4) K for **1**, **2**, and **3**, respectively, indicating the presence of moderate antiferromagnetic exchange strengths.

All three compounds exhibit a layered structure in which each Cu^{2+} (d^9) ion is connected to four nearest neighbors by a superexchange pathway through pz molecules. On the basis of the Cu site symmetry, such a structure is expected to produce square 2D magnetic layers. To test this hypothesis, the three data sets were compared to the theoretical predictions for the susceptibility of the isolated 2D $S = {}^1/_2$

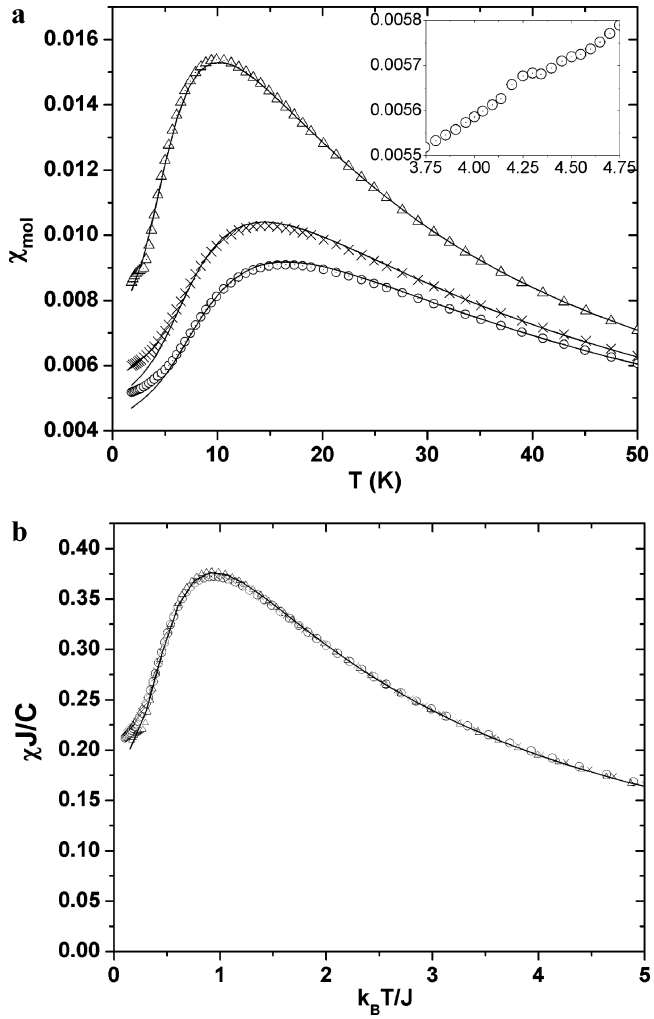

Figure 6. Comparison of powder dc magnetic susceptibility data for **1** (circles), **2** (crosses), and **3** (triangles). (a) Powder magnetic susceptibility (χ_{mol}) collected in a 0.1 T field. Solid lines represent fits to a 2D QHAF model[6a,21] with exchange strengths for **1** (17.5 K), **2** (15.3 K), and **3** (10.8 K). The inset shows the detail of the anomaly in the susceptibility of **1** near 4.3 K. (b) Same data sets are plotted in dimensionless units $J\chi_{mol}/C$ as a function of k*T*/*J*.

(20) Bonner, J. C.; Fisher, M. E. *Phys. Rev.* **1964**, *135*, A640.

antiferromagnet with Heisenberg interactions.[21] These predictions can be expressed in the form

$$\chi_{mol} = C/T[1 + (\sum_{n=1}^{5} a_n(-2J/T)^n)/(1 + \sum_{n=1}^{5} b_n(-2J/T)^n)]$$

where the coefficients a_n and b_n are given in ref 6a. In this model, the maximum susceptibility appears at a temperature $T_{max} = 0.93J/k_B$. Given that the susceptibility maxima appear at 15.9, 14.0, and 9.3 K for **1**, **2**, and **3**, respectively, the initial estimates for the exchange strengths were $J/k \approx 17$, 15, and 10 K, respectively. The application of a nonlinear squares fitting procedure, varying both the Curie constant and the exchange strengths, resulted in high-quality fits with parameters 0.426(6) cm^3·K/mol and 17.5(3) K for **1**, 0.426(6) cm^3·K/mol and 15.3(3) K for **2**, and 0.439(6) cm^3·K/mol and 10.8(3) K for **3** (solid lines in Figure 6a).

The magnetic similarities of the three compounds are illustrated in Figure 6b, in which the three susceptibility data sets have been normalized on a plot in which the vertical and horizontal axes have units of $J\chi_{mol}/C$ and T/J, respectively. The sets will be superimposable if the compounds are described by the same magnetic model. As seen in Figure 6b, there is excellent agreement between data sets for temperatures $k_BT/J > 0.5$; at lower temperatures, the data begin to rise above the predictions for the ideal 2D QHAF. The similarity of the curves in Figure 6b confirms that the 2D QHAF model is appropriate for each of them, except at the lowest temperatures, presumably near the transition to 3D long-range order.

At low temperatures, all 2D antiferromagnets undergo transitions to 3D ordered states so it was anticipated that the 2D susceptibility model would fail to describe the data at sufficiently low temperatures. Experiments were made to determine anomalies in the temperature dependence of the powder susceptibilities of **1**−**3** in an effort to determine the transitions to the magnetically ordered state, even though such studies of polycrystalline samples of Heisenberg antiferrromagnets are often insensitive[6] to the onset of magnetic order. Usually, single-crystal studies can distinguish between the susceptibilities measured parallel and perpendicular to the easy axis;[6] the temperature at which these susceptibilities separate is a good indicator of the critical temperature. The magnetization of each of the three compounds was measured every 0.05 K between 2 and 8 K in an applied field of 0.1 T. A slight anomaly was found at 4.3(1) K in the susceptibility of **1** (see Figure 6 inset); a weaker anomaly was found at 4.5(1) K for **2**, but nothing remarkable was found for **3**. We take these effects to mark the Néel temperatures of **1** and **2**.

Recent experiments sensitive to internal magnetic fields have also been used to accurately locate the Néel temperature of **1**. T_N has been determined to be 4.20(5) K by muon spin-relaxation measurements;[22] this value has also been found by elastic neutron scattering[23] experiments on deuterated single crystals of **1**. These independent measurements confirm our assumption that the susceptibility anomaly represents the ordering transition. Using these values in the previous paragraph for T_N and the respective exchange strengths of 17.5 and 15.3 K, the kT_N/J ratios are 0.24 for **1** and 0.29 for **2** and remain to be determined for **3**. Interpretation of these transition temperatures in terms of the degree of 2D isolation is found in the Discussion section. The ordering temperatures of **2** and **3** will be determined more precisely with further muon experiments.

Discussion

Every physical realization of 2D $S = {}^1/_2$ Heisenberg antiferromagnets has a finite ordering temperature as described for **1**−**3**, even though perfectly isolated 2D $S = {}^1/_2$ Heisenberg antiferromagnets enter a state of long-range order[3b] only at $T = 0$. The transitions are caused by the inevitable 3D interactions in a crystalline material, the presence of anisotropic exchange,[24] or both. The appropriate figure of merit for evaluating the degree of isolation of a low-dimensional magnet is the ratio of its ordering transition temperature to the strength of the dominant exchange interaction, k_BT_N/J. All critical transition temperatures are proportional to the primary exchange strength, so this "critical ratio" is a function of secondary interactions that drive the ordering. In the case of an ideal Heisenberg 2D magnet, k_BT_N/J would be 0, where in an ideal 3D Heisenberg magnet k_BT_N/J would be 0.945. The critical ratios for **1** and **2** are 0.24 and 0.29, respectively.

The critical ratio is correlated with the ratio of the weak 3D interaction J' to the intraplanar exchange strength J, assuming purely Heisenberg exchange. A recent Monte Carlo study[25] demonstrated that the critical ratio has a weak logarithmic dependence on J'/J; reducing J'/J from 10^{-1} to 10^{-2} to 10^{-3} only reduces the critical ratio from 0.491 to 0.326 to 0.244. The results of this study have been used to extract J'/J ratios for a selection of layered copper antiferromagnets, including **1** and **2**. These values appear in Table 4 along with comparable values for a selection of other well-characterized quasi-2D copper antiferromagnets. The information in Table 4 shows that **1** and **2** have excellent isolation of the 2D layers, second only to copper oxide compounds, which have exchange strengths 2 orders of magnitude larger.

The excellent degree of isolation can be attributed to the large separation of the layers and to the staggered stacking found in **1** and **2**. Adjacent Cu−pz planes are separated by 6.98, 6.79, and 7.00 Å for **1**, **2**, and **3**, respectively. The additional interlayer separation of 0.19 Å between **1** and **2** is attributed to the larger size of the ClO_4 counterion and may account for the decrease by a factor of 6 in the J'/J ratio.

(21) See ref 6a. Note that the equation for the susceptibility in this publication contained an error. Although the coefficients are correct, the expression for the susceptibility should be as written in the text of the present article.

(22) Lancaster, T.; Blundell, S. J.; Brooks, M. L.; Baker, P. J.; Pratt, F. L.; Manson, J. L.; Connor, M. M.; Xiao, F.; Landee, C. P.; Chaves, A.; Soriano, S.; Novak, M. A.; Papageorgiou, T.; Bianchi, A.; Herrmannsdoerfer, T.; Wosnitza, J.; Schlueter, J. A. *Phys. Rev. B: Condens. Matter Mater. Phys.*, in press.
(23) Kenzlemann, M., private communication.
(24) de Jongh, L. J.; Miedema, A. R. *Adv. Phys.* **2001**, *50*, 947.
(25) Yasuda, C.; Todo, S.; Hukushima, K.; A lot, F.; Keller, M.; Troyer, M.; Takayama, H. *Phys. Rev. Lett.* **2005**, *94*, 217201.

Table 4. Comparison of Magnetic Parameters for Selected 2D $S = {}^1/_2$ Heisenberg Antiferromagnets[a]

compound	T_N (K)	J/k (K)	kT_N/J	J'/J	ref
$(5CAPH)_2CuBr_4$	5.08	8.5	0.60	0.25	6
$CuF_2 \cdot 2H_2O$	10.9	26	0.42	0.048	48
copper formate tetrahydrate	16.5	≈70	0.24	8×10^{-4}	49
La_2CuO_4	310	1500	0.21	2×10^{-4}	50
$Sr_2CuO_2Cl_2$	251	1450	0.17	2×10^{-5}	51
$[Cu(pz)_2(HF_2)]BF_4$	1.54	5.7	0.27	2.3×10^{-3}	26
$Cu(pz)_2(ClO_4)_2$	4.2	17.5	0.24	8.0×10^{-4}	this work
$Cu(pz)_2(BF_4)_2$	4.5	15.3	0.29	4.6×10^{-3}	this work
$[Cu(pz)_2(NO_3)](PF_6)$	3.05	10.8	0.28		this work

[a] The ratios of interlayer to intralayer exchange (J'/J) are based upon the results of Yasuda et al.[24]

For **1** and **2**, adjacent layers are offset with respect to one another so the interlayer Cu−Cu distance becomes 8.54 and 7.92 Å, respectively. Not only does the offset increase the interlayer Cu−Cu distance, it provides for a near-cancellation of interlayer exchange J'. Each copper ion is situated equidistant from four symmetry-equivalent copper sites of the layer above, of which two are spin up and two are spin down. Whatever the sign or strength of the interaction J', the net interaction between layers vanishes to first order in J', yielding excellent 2D isolation of the layers. The same cancellation is found in the well-known copper oxide La_2CuO_4 (Table 4).

The interlayer Cu−Cu separation in **3** is 1.5 Å shorter than that in **1** and 0.92 Å shorter than that found in **2**, due to its *I*4*mcm* structure, which contains NO_3 anions linking copper cations in adjacent Cu−pz layers (Figure 5). The NO_3 group provides a bonding superexchange pathway between layers. In addition, there is no offset of adjacent layers in **3** and consequently no cancellation of interlayer coupling. It can therefore be anticipated that there will be a stronger interlayer interaction in this material, which would manifest itself in the largest value of kT_{min}/J for this family of compounds.

The high symmetry of this complex should nevertheless keep the interlayer exchange low. The unpaired electron of the Cu(II) ion lies in the $d_{x^2-y^2}$ orbital with the lobes oriented toward the pyrazine N atoms. It will have minimal spin density out of the plane, and the overlap of the d orbital with the nitrate O atoms should be minimal. The good magnetic isolation of the layers should be preserved. This is found to be the case in the tetragonal complex $[Cu(pz)_2(HF_2)]BF_4$ in which the HF_2 anions bridge adjacent planes;[26] yet the critical ratio is only 0.27, corresponding to a low J'/J ratio of 2.3×10^{-3}.

The three Cu−pz layers reported here are characterized by Cu sites coordinated to four pz molecules by short (2.05−2.07 Å) Cu−N bonds, with the axial sites occupied by more distant (2.3−2.4 Å) ligands. Five other compounds with the same $Cu(pz)_2$ stoichiometry have been reported,[26−30] but only three contain analogous Cu−pz layers as described below (see Table 5 for a comparison of the structural parameters).

Table 5. Comparison of Magnetostructural Parameters for Copper Bispyrazine Antiferromagnetic Layers[a]

	compound				
	1	**2**	**3**	HF_2	V_6O_{16}
ref	this work	this work	this work	26	30
T, X-ray, K	163	160	163	293	221
space group	*C*2/*c*	*C*2/*m*	*I*4/*mcm*	*P*4*nbm*	*C*2/*c*
a, Å	14.072	9.692	9.7093	9.690	22.121
b, Å	9.786	9.736	9.7093	6.6901	9.309
c, Å	9.781	7.916	14.006	6.619	10.014
β, deg	96.458	120.920	90	90	112.90
Cu−N1, Å	2.071	2.052	2.042	2.040	2.026
Cu−N2, Å	2.074	-	-	-	2.031
Cu−X, Å	2.374	2.338	2.413	2.207	2.236
Cu−X−Y, deg	159.9	161.9	159.6	180	143.1
tilt, deg	62.8, −69.1	67.4	61.4	59.4	61.3, 45.9
J/k, K	17.5	15.3	10.8	5.7	8.5

[a] Cu−X is the distance from the Cu atom to the nearest atom in the axial site. Cu−X−Y is the angle formed by the Cu, the nearest, and the next-nearest atoms in the axial site. "Tilt" is the angle between the mean plane of the pz ring and the mean plane of the Cu(II) ion and its four closest bonded atoms.

$[Cu(pz)_2(HF_2)]BF_4$ is structurally very similar to **3**.[26] Its room-temperature structure[31] contains a 4-fold symmetry axis (space group *P*4/*nbm*) reflecting four identical Cu−N bonds of 2.040 Å (2.042 Å in **3**); each Cu atom also has semicoordinate Cu−F bonds in the axial sites (2.207 Å), with the linear HF_2 ions bridging adjacent layers in a manner similar to which adjacent Cu−pz layers are linked by the NO_3 ions in **3** (Cu−O = 2.413 Å). The in-plane unit cell distances are nearly identical for the two structures (9.690 Å for the HF_2 complex and 9.709 Å for **3**), but the interlayer separation is considerably greater, as expected for the NO_3-bridged complex (7.003 Å for **3** and 6.619 Å for $[Cu(pz)_2(HF_2)]BF_4$). The powder susceptibility data for $[Cu(pz)_2(HF_2)]BF_4$ show a rounded maximum near 5.5 K and can be described by the 2D QHAF model with $J/k = 5.7$ K. Muon spin-relaxation measurements and specific-heat data demonstrate the existence of an ordering temperature at 1.54 K, yielding a critical ratio kT_N/J for this compound of 0.27.

$Cu(pz)_2V_6O_{16} \cdot (H_2O)_{0.22}$ contains $Cu(pz)_2^{2+}$ square nets with the copper coordination sphere consisting of four short Cu−N bonds, two each of 2.026 and 2.031 Å, plus longer axial bonds to two O atoms of 2.236 Å.[30] The O atoms are part of the buckled $V_6O_{16}^{2-}$ layers that separate the cu−pz planes. There are two different pz tilt angles of 61.3° and 45.9°, as permitted by the *C*2/*c* space group. The magnetic susceptibility shows a rounded maximum near 8 K. The data were not fit to a 2D model, but based on the relationship for the 2D QHAF model that the temperature of the maximum susceptibility occurs at 93% of the exchange strength, the exchange strength of this compound can be estimated to be around 8.5 K. There is no information regarding its ordering temperature.

(26) Manson, J. L.; Conner, M. M.; Schlueter, J. A.; Lancaster, T.; Blundell, S. J.; Brooks, M. L. Pratt, F. L.; Papageorgiou, T.; Bianchi, A. D.; Wosnitza, J.; Wangbo, M.-H. *Chem. Commun.* **2006**, *1*−*3*, 1.
(27) Haynes, J. S.; Rettig, S. J.; Sams, J. R.; Thompson, R. C.; Trotter, J. *Can. J. Chem.* **1987**, *65*, 420−426.
(28) Halasayamani, P.; Heier, K. R.; Willis, M. J.; Stern, C. L.; Poeppelmeier, K. R. *Z. Anorg. Allg. Chem.* **1996**, *622*, 479.
(29) Heier, K. R.; Norquist, A. J.; Halasyamani, P. S.; Duarte, A.; Stern, C. L.; Poeppelmeier, K. R. *Inorg. Chem.* **1999**, 38, 762.
(30) Maggard, P. A.; Boyle, P. D. *Inorg. Chem.* **2003**, *42*, 4250.
(31) Structural transitions occur in $[Cu(pz)_2(HF_2)]BF_4$ below 160 K, but the low-temperature structure remains unknown. Manson, J., personal communication.

$Cu(pz)_2(WO_2F_4)\cdot(pz)(H_2O)$ also contains Cu−pz layers, but no magnetic data are available for it.[29] This compounds exists in two high-symmetry polymorphs (**I**, space group *I*4/*mcm*; **II**, space group *P*4/*mmm*), each containing identical uniform copper−pyrazine layers. The Cu−pz bonds are shorter (2.062 Å in both polymorphs), with the axial sites occupied by more distant atoms from the bridging WO_2F_4 groups (2.248 Å is the average distance). The axial sites of the coppers are disordered, with 50% occupancy by both O and F atoms. The layers lie directly over one another, bridged by the WO_2F_4 anions, analogous to the stacked layers in **3**.

Two other compounds, $Cu(pz)_2(CH_3SO_3)_2$[27] and $Cu(pz)_2(NbOF_5)_2\cdot(pz)(H_2O)$,[28] have the same stoichiometry as **1**−**3** but do not contain 2D Cu−pz planes. Each compound contains two different Cu sites, the first having four short bonds to N and two to the counterion, whereas the second site has two short N atom bonds, two short bonds to the counterion and two long N atom bonds. These compounds behave magnetically as one-dimensional systems, with $Cu(pz)_2(CH_3SO_3)_2$ having an exchange strength of 10.8 K.[27] Only a weak negative Curie−Weiss temperature of −3.0 K was reported for $Cu(pz)_2(NbOF_5)_2\cdot(pz)(H_2O)$.[28]

The five compounds **1**−**3**, $[Cu(pz)_2(HF_2)]BF_4$, and $Cu(pz)_2V_6O_{16}\cdot(H_2O)_{0.22}$ have very similar cu−pz antiferromagnetic layers (Table 5) but have exchange strengths that vary by a factor of 3, from 5.7 K for $[Cu(pz)_2(HF_2)]BF_4$ to 17.5 K for **1**. There are no obvious magnetostructural correlations that explain this variation. The compound with the shortest Cu−N bond between the Cu atom and the pz ring is $Cu(pz)_2V_6O_{16}\cdot(H_2O)_{0.22}$ (Cu−N = 2.026 Å, 2.031 Å), yet it has an exchange strength only half that of the low-temperature phase of **1** (Cu−N = 2.071 and 2.074 Å). It has been proposed[8b] that the strength of the interaction through the pz molecule is related to the tilt angle between the pz plane and the Cu coordination plane, as the overlap between the ring π electrons and Cu d orbital was varied. However, no systematic variation between the tilt angle and exchange strength is observed for these compounds. Studies of the family of $Cu(sub\text{-}pz)(NO_3)_2$ antiferromagnetic chains (sub-pz = methyl- or dimethyl-substituted pyrazine)[8c] showed that the observed variations of exchange strength were more closely related to slight changes in the coordination geometry of the Cu site, with alterations of the tilt angle secondary. The π−d orbital overlap model suggests that the strength of the superexchange interaction will be strongest when the unpaired electron occupies only the $d_{x^2-y^2}$ state, with no mixing of the d_{z^2} state. This configuration is found only for the tetragonal compound **3**, but this compound has one of the weaker exchange strengths. Both **1** and **2** are monoclinic with lower Cu site symmetries but have higher exchange strengths. The explanation for the varying interactions strengths found in the Cu−pz layer is not clear at this time.

The family of compounds $M(pz)_2X_2$ also contains non-Cu members, where M is a 3d transition metal dication (Mn, Fe, Co, Ni) and X is a halide or pseudohalide (Cl, Br, NCS). These compounds also form $M(pz)_2$ layers similar to those found in **1**−**3**, but when the axial ligands are Cl or Br, the exchange strengths are always weak, frequently less than one wavenumber. The structure of $Co(pz)_2Cl_2$ has been determined[32] and shown to consist of infinite $Co(pz)_2$ layers with a square-planar $Co-N_4$ coordination completed to a nearly undistorted square bipyramid by the two Cl ligands (Co−N = 2.182 Å, Co−Cl = 2.406 Å, Cl−Co−N = 89.6°, pz tilt angle = 46.5°). The corresponding iron(II), cobalt(II), and nickel(II) pyrazine dibromide compounds are isostructural,[33] with, in every case, the coordination consisting of an elongated 4 + 2 configuration. The pz tilt angles are either 48° (Fe, Ni) or 47° (Co).

The two ferrous halide compounds have been studied magnetically[33,34] and have been shown to have effective moments that decrease below 50 K, but no ordering transitions have been detected down to helium temperatures. Due to the complex dependence of the moment of a Fe(II) ion in distorted octahedral geometry, no modeling has been possible for the susceptibility. Weak interactions have been found to exist in the cobalt complexes, as the cobalt chloride and bromide analogues undergo transitions to long-range order[35] at temperatures of 0.85 and 0.66 K, respectively. The magnetic and specific-heat data above the critical temperatures could be described with exchange strengths of $2J_{Cl}/k = -0.84$ K and $2J_{Br}/k = -0.66$ K based on a 3D *XY* model. It is not clear how the 3D model is commensurate with the known structure. Magnetic studies of $Ni(pz)_2Cl_2$[36] and $Ni(pz)_2Br_2$[33] showed the susceptibility to be dominated by single-ion effects ($D \approx 5-7$ cm^{-1}) with antiferromagnetic interactions no more than 0.1 cm^{-1}.

Replacing the true halides by thiocyanate in the axial sites leads to important changes in the crystal structure with subsequent enhancement of the exchange interactions. The crystal structures of $Mn(pz)_2(NCS)_2$,[37] $Fe(pz)_2(NCS)_2$,[38] and $Co(pz)_2(NCS)_2$[39] all consist of parallel sheets of square arrays of M(II) atoms bridged by pyrazines, with the thiocyanate ions occupying the axial positions and coordinated by the nitrogens. These structures differ from those with halides described above in that the NCS^- groups are more strongly coordinated than the pyrazines, leading to a compressed octahedral environment for the metals. The M−NCS and M−N(pz) bonds are 2.139 and 2.317 Å, 2.050 and 2.210 Å, and 2.071 and 2.246 Å for the Mn, Fe, and Co analogues, respectively. Consequently, the pyrazine rings increase their tilt angles to 66.5° for the Mn compound and 64° for the Fe and Co compounds.

$Fe(pz)_2(NCS)_2$ has undergone the most extensive magnetic investigation of the thiocyanate family. In the initial report

(32) Gairing, C.; Lentz, A.; Groβe, E.; Haeidl, M.; Walz, L. *Z. Kristallogr.* **1996**, *211*, 804.
(33) James, M. *Aust. J. Chem.* **2002**, *55*, 219.
(34) Haynes, J. S.; Sams, J. R.; Thompson, R. C. *Inorg. Chem.* **1986**, *25*, 3740.
(35) Carlin, R. L.; Carnegie, D. W., Jr.; Bartolome, J.; Gonzalez, D.; Floria, L. M. *Phys. Rev. B: Condens. Matter Mater. Phys.* **1985**, *32*, 7476−82.
(36) Otieno, T.; Thompson, R. C. *Can. J. Chem.* **1995**, *73*, 275.
(37) Näther, C.; Greve, J. *J. Solid State Chem.* **2003**, *176*, 259−265.
(38) Real, J. A.; De Munno, G.; Munoz, M. C.; Julve, M. *Inorg. Chem.* **1991**, *30*, 2701−2704.
(39) Lu, J.; Paliwala, T.; Lim, S. C.; Yu, C.; Niu, T.; Jacobson, A. J. *Inorg. Chem.* **1997**, *36*, 923.

on this compound,[40] its susceptibility was found to display a rounded maximum near 8 K; the data could be fit to the model of a 2D, $S = 2$ Heisenberg model with $2J/k = -1.3$ K, although the data near the peak were not well described with this model. Mössbauer spectra revealed the presence of an ordering temperature between 7 and 9 K even though there is no distinct feature in the susceptibility in this temperature range other than the low-dimensional maximum. Real et al.[38] repeated the magnetic measurements and refit their data to the same model with a molecular field correction for interlayer exchange. Their parameters were similar ($2J/k = -1.6$ K and $2z'J' = -1.4$ K), but the quality of the fit remained poor. A recent[41] study of $Fe(pz)_2(NCS)_2$ used Mössbauer spectra, specific-heat, and magnetic measurements as well as neutron powder diffraction and inelastic neutron scattering to characterize the nature of the phase transition and the magnetic structure. The ordering temperature was found to be $T_N = 6.67$ K by specific-heat measurements. In addition, the magnetic specific heat could be described both above and below the transition temperature as arising from a 2D Ising model with an exchange strength of $2J/k = 2.95$ K. The Ising nature of the magnetic exchange explains the inability of the Heisenberg models to explain the behavior of the susceptibility. This exchange strength is the largest yet known for any non-Cu−pz layer but is still a factor of 5 smaller than the exchange strength of **1** or **2**.

An analysis of the powder susceptibilities of other members of the thiocyanate family[42] found decreases in the magnetic moments at low temperatures, although no maxima were found for the susceptibilities. With the employment of 2D Heisenberg models with different spin values, the data for $Mn(pz)_2(NCS)_2$, $Co(pz)_2(NCS)_2$, and $Ni(pz)_2(NCS)_2$ could be modeled with approximate exchange strengths of 0.3, 1.4, and 1.2 K, respectively, although these models ignore important single-ion effects for the Co and Ni analogues that can cause significant decreases in the effective moments. As such, these values probably represent upper limits for the interactions.

Efforts to understand superexchange interaction strengths of 3d metals bridged by pyrazine and other diazine molecules date back 30 years. In addition to the work by Hatfield and co-workers mentioned above, Hoffmann et al.[43] used the extended Hückel molecular orbital approach to predict that pyrazine would be an effective superexchange ligand acting through a σ-type pathway. Dimeric compounds such as $[Cu_2(tren)_2(bridge)](ClO_4)_4$ (tren = 2, 2′,2″-triaminotriethylamine, bridge = pz or 1,4-diazabicyclo[2.2.2]octane, Dabco) were synthesized[44] to test this conjecture since the copper coordination places the unpaired electron in the d_{z^2} orbital, pointing directly at the nitrogen lone-pair orbitals of the bridging group. The Dabco ligand was thought to be a particularly good test because it contained only σ bonds. However, magnetic studies showed the exchange in the Dabco dimer to be indistinguishable from zero, whereas a weak exchange is found for the pyrazine-bridged dimer ($|J|/k = 4.6$ K). There has been no theory of pyrazine-mediated exchange with predictive power in the intervening 3 decades and no quantitative way to understand the variation of superexchange strengths seen in **1**−**3**.

Recent applications of density functional theory have led to a first-principles, bottoms-up approach that enables the computation of macroscopic magnetic properties, such as exchange strengths or magnetic susceptibilities, of a crystal from only a knowledge of its crystal structure.[45] This approach has been used to examine the magnetic properties of three purely organic nitronyl nitroxide crystals[46] plus two antiferromagnetic spin ladders assembled by close bromide−bromide contacts between $CuBr_4$ dianions.[47] With the use of this approach, it is possible to examine the dependence of an exchange strength upon a structural parameter such as the Cu−N bond length or the pyrazine tilt angle. We are currently investigating these possibilities.

Conclusion

The planar coordination polymer structure of the $[Cu(pz)_2]^{2+}$ family can be maintained with modest changes in the gegenion. The structures of the ClO_4^- (**1**) (room temperature) and BF_4^- (**2**) (163 K) complexes are isomorphous. Even in the case of the mixed-anion complex **3**, the 2D $[Cu(pz)_2]^{2+}$ unit is maintained. A nondestructive phase change is observed in **1** and **1a** which, although it does reduce the symmetry at the metal center, does not appear to affect the nature of the magnetic interactions significantly. Compound **2** does not show the analogous phase change down to 163 K, but lower temperature experiments are in progress. The magnetic exchange for all three compounds, estimated from data in Figure 5, is found to be moderate, falling in a range from 10 to 18 K.

Acknowledgment. The Clark University Quantum Design MPMS-XL SQUID magnetometer was purchased with

(40) Haynes, J. S.; Kostikas, A.; Sams, J. R.; Simopoulos, A.; Thompson, R. C. *Inorg. Chem.* **1987**, *26*, 2630.
(41) Bordallo, H. N.; Chapon, L.; Manson, J. L.; Hernández-Valasco, J.; Ravot, D.; Reiff, W. M.; Argyriou, D. N. *Phys. Rev. B: Condens. Matter Mater. Phys.* **2004**, *69*, 224405.
(42) Lloret, F.; Julve, M.; Cano, J.; De Munno, G. *Mol. Cryst. Liq. Cryst.* **1999**, *334*, 569.
(43) Hay, P. J.; Thibeault, J. C.; Hoffmann, R. *J. Am. Chem. Soc.* **1975**, *97*, 4884.
(44) Haddad, M. S.; Hendrickson, D. N.; Cannady, J. P.; Drago, R. S.; Bieksza, D. S. *J. Am. Chem. Soc.* **1979**, *104*, 898.
(45) (a) Deumal, M.; Bearpark, M. J.; Robb, M. A.; Pontillon, Y.; Novoa, J. J. *Chem.—Eur. J.* **2004**, *10* (24), 6422. (b) Deumal, M.; Mota, F.; Bearpark, M. J.; Robb, M. A.; Novoa, J. J. *Mol. Phys.* **2006**, *104*, 857. (c) Jornet, J.; Deumal, M.; Ribas-Arino, J.; Bearpark, M. J.; Robb, M. A.; Hicks, R. G.; Novoa, J. J. *Chem.—Eur. J.* **2006**, *12*, 3995.
(46) Deumal, M.; Bearpark, M. J.; Novoa, J. J.; Robb, M. A. *J. Phys. Chem. A* **2002**, *106*, 1299.
(47) (a) Deumal, M.; Giorgi, G.; Robb, M. A.; Turnbull, M. M.; Landee, C. P.; Novoa, J. J. *Eur. J. Inorg. Chem.* **2005**, *4697*. (b) Shapiro, A.; Landee, C. P.; Turnbull, M. M.; Jornet, J.; Deumal, M.; Novoa, J. J.; Robb, M. A.; Lewis, W. *J. Am. Chem. Soc.* **2007**, *129*, 952.
(48) Abrahams, S. C. *J. Chem. Phys.* **1962**, *36*, 56.
(49) Clarke, S. J.; Harrison, A.; Mason, T. E.; McIntyre, G. J.; Visser, D. *J. Phys.: Condens. Matter* **1992**, *4*, L71.
(50) Endoh, Y.; Yamada, K.; Birgeneau, R. J.; Gabbe, D. R.; Jenssen, H. P.; Kastner, M. A.; Peters, C. J.; Picone, P. J.; Thurston, T. R.; Tranquada, J. M.; Shirane, G.; Hidaka, Y.; Oda, M.; Enomoto, Y.; Suzuki, M.; Murakami, T. *Phys. Rev. B: Condens. Matter Mater. Phys.* **1988**, *37*, 7443.
(51) Greven, M.; Birgeneau, R. J.; Endoh, Y.; Kastner, M. A.; Keimer, B.; Matsuda, M.; Shirane, G.; Thurston, T. R. *Phys. Rev. Lett.* **1994**, *72*, 1096.

the assistance of the NSF (through Grant IMR-0314773) and the Kresge Foundation. We thank Professor Joe Budnick (University of Connecticut) for the use of his magnetometer and Fan Xiao for his assistance with data collection and preparation of figures.

Supporting Information Available: Three CIF files. This material is available free of charge via the Internet at http://pubs.acs.org.

IC0621392